JGR Biogeosciences

RESEARCH ARTICLE
10.1029/2018JG004650

Special Section:
Biogeochemistry of Natural Organic Matter

The Potential Hidden Age of Dissolved Organic Carbon Exported by Peatland Streams

Joshua F. Dean[1,2,3], Mark H. Garnett[2], Evangelos Spyrakos[1], and Michael F. Billett[1]

[1]Biological and Environmental Sciences, University of Stirling, Stirling, UK, [2]NERC Radiocarbon Facility, East Kilbride, UK, [3]Department of Earth Sciences, Vrije Universiteit Amsterdam, Amsterdam, The Netherlands

Key Points:
- Using an incubation experiment, DOC from a peatland stream was decomposed to CO_2, measuring the ^{14}C content of both
- The bulk DOC pool was modern, but labile carbon >1,000 years BP was also detected
- Bulk radiocarbon dating of peatland stream DOC is an insensitive method for detecting old carbon

Supporting Information:
- Supporting information S1

Correspondence to:
J. F. Dean,
joshua.dean@liverpool.ac.uk

Citation:
Dean, J. F., Garnett, M. H., Spyrakos, E., & Billett, M. F. (2019). The potential hidden age of dissolved organic carbon exported by peatland streams. *Journal of Geophysical Research: Biogeosciences*, *124*, 328–341. https://doi.org/10.1029/2018JG004650

Received 13 JUN 2018
Accepted 26 JAN 2019
Accepted article online 2 FEB 2019
Published online 22 FEB 2019

Author Contributions:
Conceptualization: Joshua F. Dean, Michael F. Billett
Data curation: Mark H. Garnett, Evangelos Spyrakos, Michael F. Billett
Formal analysis: Joshua F. Dean, Mark H. Garnett
Funding acquisition: Mark H. Garnett, Michael F. Billett
Methodology: Joshua F. Dean, Mark H. Garnett, Evangelos Spyrakos, Michael F. Billett
Resources: Michael F. Billett
Supervision: Mark H. Garnett
(continued)

Abstract Radiocarbon (^{14}C) is a key tracer for detecting the mobilization of previously stored terrestrial organic carbon (C) into aquatic systems. Old C (>1,000 years BP) may be "masked" by postbomb C (fixed from the atmosphere post-1950 CE), potentially rendering bulk aquatic dissolved organic C (DOC) ^{14}C measurements insensitive to old C. We collected DOC with a modern ^{14}C signature from a temperate Scottish peatland stream and decomposed it to produce CO_2 under simulated natural conditions over 140 days. We measured the ^{14}C of both DOC and CO_2 at seven time points and found that while DOC remained close to modern in age, the resultant CO_2 progressively increased in age up to 2,356 ± 767 years BP. The results of this experiment demonstrate that the bulk $DO^{14}C$ pool can hide the presence of old C within peatland stream DOC export, demonstrating that bulk $DO^{14}C$ measurements can be an insensitive indicator of peatland disturbance. Our experiment also demonstrates that this old C component is biologically and photochemically available for conversion to the greenhouse gas CO_2, and as such, bulk $DO^{14}C$ measurements do not reflect the ^{14}C signature of the labile organic C pool exported by inland water systems more broadly. Moreover, our experiment suggests that old C may be an important component of CO_2 emissions to the atmosphere from peatland aquatic systems, with implications for tracing and modeling interactions between the hydrological and terrestrial C cycles.

Plain Language Summary The introduction of old carbon previously stored in soils for thousands of years into rivers can increase the net flux of greenhouse gases to the atmosphere, impacting global climate. This is because rivers transport the equivalent of one third of human carbon emissions annually from land to the oceans. Much river-borne carbon is plant and soil (organic) matter that can decompose during transport, releasing greenhouse gases to the atmosphere. Radiocarbon dating can reveal the age of river-borne carbon, but previous measurements may have underestimated the age of carbon released into rivers by not considering the potential for old carbon hidden within individual bulk water samples. Using an incubation experiment, we demonstrate that dissolved organic carbon from a Scottish peatland stream that would be considered modern in age using traditional bulk radiocarbon dating can readily decompose to produce carbon dioxide with an old radiocarbon signature up to ~2,500 years old. This demonstrates that radiocarbon dating of bulk riverine dissolved organic carbon can hide the presence of old carbon. Furthermore, these results indicate that old carbon may be more common in the global carbon cycle than previously thought, with important implications for our understanding and modeling of peatland ecosystems.

1. Introduction

Radiocarbon (^{14}C) analysis of dissolved organic carbon (DOC) has become a key tool over the past ~30 years for detecting the mobilization of C into streams as a signal of environmental change (Butman et al., 2015). Since the Last Glacial Maximum ~20,000 years ago, up to 620 Pg of C has accumulated in peatland soils around the globe (Page et al., 2011). These soils are vulnerable to environmental disturbance, which can impact terrestrial C loss through both greenhouse gas emissions (CO_2 and CH_4) and aquatic export of DOC, particulate organic C(PIC), and dissolved and particulate inorganic C (Evans et al., 2014; Hemes et al., 2018). As an environmental indicator of peatland C loss, ^{14}C is particularly effective for detecting the lateral export of DOC containing old C (defined here as >1,000 years BP) released as a result of land clearance, drainage, and/or climate change (Figure 1). In pristine peatland catchments or those affected by only limited disturbance, 87–90% of $DO^{14}C$ values are modern (Figure 1). This matches what is seen at the global scale, with most studies finding predominantly modern $DO^{14}C$ exported by rivers (Marwick

Writing - original draft: Joshua F. Dean
Writing – review & editing: Mark H. Garnett, Michael F. Billett

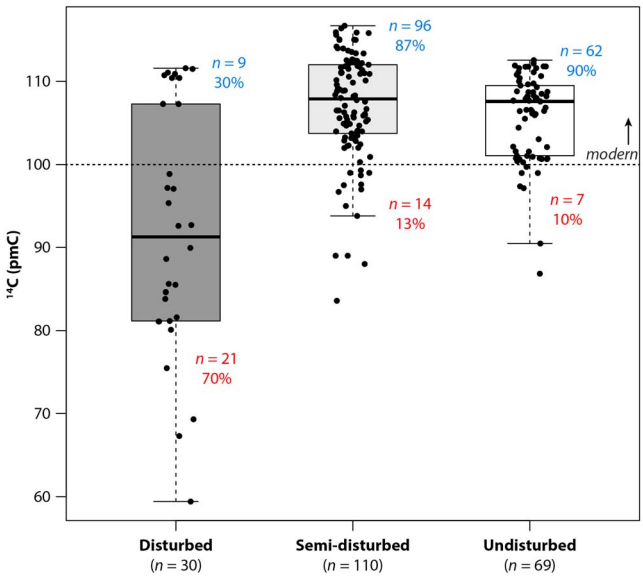

Figure 1. ^{14}C values for dissolved organic carbon exported from peatland catchments that have been heavily disturbed (e.g., by drainage; Moore et al., 2013), semidisturbed (e.g., by long-term impacts from minor human activity; Billett et al., 2007), or relatively undisturbed by human activity (Aiken et al., 2014; Dean, van der Velde, et al., 2018; Campeau et al., 2017; Hulatt, Kaartokallio, Oinonen, et al., 2014; Hulatt, Kaartokallio, Asmala, et al., 2014; Ledesma et al., 2015; Leith et al., 2014; Marwick et al., 2015; Müller et al., 2015; Stimson et al., 2017a, 2017b). Modern $DO^{14}C$ values plot above the dotted line; the number of modern values for each catchment type is shown in blue, and the number of values older than modern is shown in red (total $n = 209$; see supporting information for data sources).

et al., 2015). Conversely, 70% of $DO^{14}C$ values from extensively disturbed peatland catchments show a clear aged signal (Figure 1).

In peatland catchments, stream DOC is the main form of lateral C export (often 50–80%; Billett et al., 2010), incorporating C from multiple terrestrial sources and soil depths within its source area (Aiken et al., 2014; Evans et al., 2014; Leach et al., 2016). In most peatland aquatic $DO^{14}C$ studies to date, predominantly in the UK, North America, Scandinavia, Malaysia, and Indonesia, $DO^{14}C$ concentrations are generally modern (i.e., with a radiocarbon content of >100 percent modern C [pmC]; Figure 1), despite inputs from deep organic soil layers where the oldest C is stored, potentially 3,000–6,000 years BP or older (Dargie et al., 2017; Evans et al., 2014; Garnett & Hardie, 2009; Garnett et al., 2011; Hulatt, Kaartokallio, Oinonen, et al., 2014; Leith et al., 2014; Moore et al., 2013; Tipping et al., 2010). The notable exceptions to this are the disturbed sites shown in Figure 1. Attempts to reconcile the multiple sources contributing to bulk aquatic $DO^{14}C$ samples have involved matching the measured ^{14}C content to the predicted soil organic matter ^{14}C profiles in their catchment area (Figure 2; Dean, van der Velde, et al., 2018; Evans et al., 2014; Moore et al., 2013; Raymond et al., 2007). Soil ^{14}C profiles are affected by a peak in ^{14}C concentrations caused by atmospheric nuclear bomb testing (Dutta, 2016). This results in a substantial pool of highly ^{14}C-enriched C in upper soil profiles that can skew the ^{14}C signature of the bulk DOC pool, essentially masking any old C (Raymond & Bauer, 2001). For example, a "modern" DOC sample with a ^{14}C concentration of 102 pmC could contain 2% old C, yet a slightly older DOC sample with a ^{14}C concentration of 97 pmC can potentially comprise 14% old C; at 90 pmC, old C could contribute as much as 38% to the total DOC pool (Figure 2).

During transport and storage in inland water systems, DOC can decompose to produce CO_2, contributing to the supersaturation of many global freshwaters with CO_2 (Catalán et al., 2016; Cole et al., 2007; McCallister & del Giorgio, 2012). On their own, CO_2 emissions from inland waters are equivalent to ~19% of current anthropogenic emissions (Holgerson & Raymond, 2016; Raymond et al., 2013). In the USA, it is estimated that 28% of the CO_2 emitted from inland waters is from the photodecomposition and microbial decomposition of DOC during aquatic transport (Hotchkiss et al., 2015); in UK peatlands, 12–18% of exported DOC may be lost in this way (Dawson et al., 2001). DOC decomposition occurs via both microbial respiration (Logue et al., 2016; Raymond & Bauer, 2001), and photo-oxidation (Köhler et al., 2002; Pickard et al., 2017). Microbial respiration is often considered to be the primary process for the conversion of DOC to CO_2, and

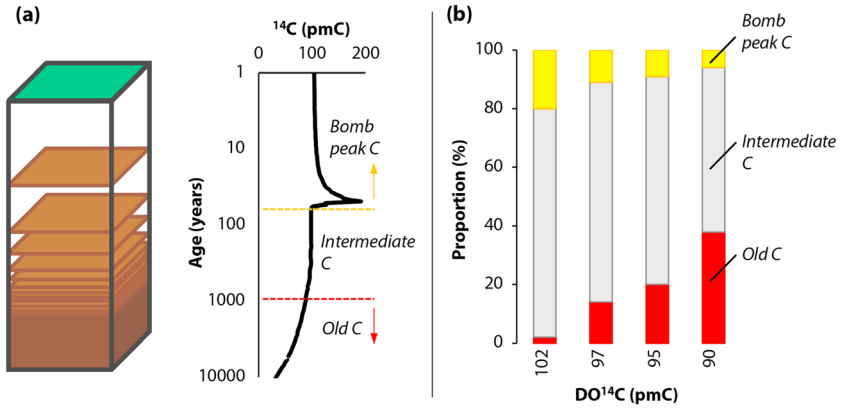

Figure 2. (a) The assignment of atmospheric ^{14}C ages to a soil profile in an exponential distribution (Dean, van der Velde, et al., 2018; Hua et al., 2013; Levin et al., 2013; Reimer et al., 2013). (b) The potential contribution of C of different ages to example peatland fluvial DO^{14}C values (in percent modern C [pmC]) based on inputs from the soil ^{14}C profile in (a).

many investigations into aquatic DOC decomposition focus on this process (Dean, van Hal, et al., 2018; Vonk et al., 2015). However, photo-oxidation can stimulate or inhibit the microbial respiration of DOC through partial oxidation and can also directly oxidize DOC to CO_2, so both photo-oxidation and microbial respiration are important for the decomposition of inland water DOC (Cory & Kling, 2018). Organic C (OC) carried by inland waters can also be buried and stored in sediments in the form of POC (Wohl et al., 2017). POC is often defined as OC particles larger than 0.7 μm, as opposed to DOC, which is defined here as <0.7 μm. POC can form through the biological and physical flocculation of smaller OC and mineral molecules and can contain significant amounts of heterotrophic and autotrophic biomass from respiration of OC (i.e., generating free CO_2 in the water) and photosynthesis (i.e., fixing free CO_2), respectively (Hunter et al., 2016).

Despite the importance of microbial processes for regulating the fate of C mobilized from temperate peatlands, there is a clear disconnect between the ^{14}C age of stream DOC and CO_2 (Billett et al., 2007). DOC is predominantly modern (Figure 1), while the majority (62%) of $^{14}CO_2$ values are older (average $^{14}CO_2$ concentration = 96.5 ± 6.5 pmC; ±1σ; n = 92; Billett et al., 2006, 2007, 2012; Garnett et al., 2012, 2013; Garnett, Billett, et al., 2016; Leith et al., 2014; Tittel et al., 2013). Figure 2 shows that bulk DO^{14}C samples have the potential to contain a wide range of C ages from modern through to several thousand years old. If components of a certain age in the DOC pool are preferentially decomposed to CO_2, then this could explain the disparity between in situ DO^{14}C and $^{14}CO_2$ measurements (Galy & Eglinton, 2011; Loh et al., 2006; McCallister & del Giorgio, 2012). Aquatic CO_2 may also be generated from source material in the soil zone that is of a different age to the DOC pool, or even ^{14}C-dead (0 pmC) geological sources, further complicating bulk $^{14}CO_2$ signals (Billett et al., 2007; Dean, van der Velde, et al., 2018). This suggests that DO^{14}C measurements are not a good proxy for the age of CO_2 emitted from inland water systems.

Here we present an incubation experiment isolating the CO_2 released from the combined photodecomposition and microbial decomposition of peatland stream DOC. We tested the hypothesis that there is an old C component hidden within modern peatland stream DOC pools and that this old C is available for decomposition through natural in-stream processing to CO_2. We collected a large bulk ^{14}C-modern DOC sample from a temperate peatland stream in the UK with the potential to receive old C from the deep peat soils within its catchment. We incubated this sample under a simulated day-night cycle for 140 days to represent the interaction between photodecomposition and microbial decomposition of the stream DOC pool. We measured the ^{14}C of DOC and CO_2 concurrently during the incubation and POC formed by microbial growth at the end of the experiment.

2. Materials and Methods

2.1. Field Sampling

The DOC-rich water for incubation was collected on 17 March 2015 from Black Burn, a first-order stream draining a 3.4-km^2 catchment of Auchencorth Moss peatland (55°48′N, 03°15′W) in central Scotland

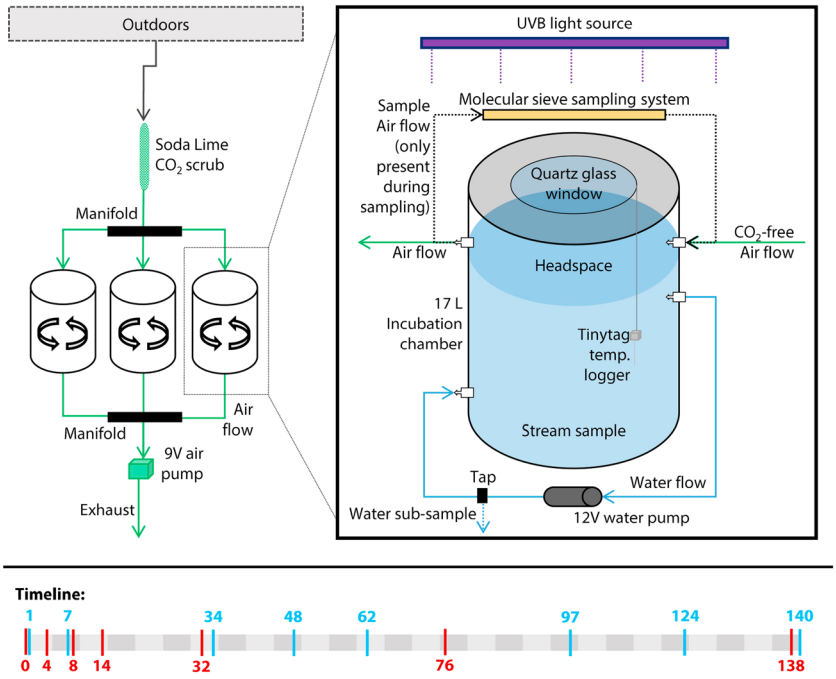

Figure 3. Incubation chamber design. (left) The schematic of all three chambers connected via an outside air line and a CO_2 scrub (soda lime). (right) The design of each of the chambers used for the stream water incubations and headspace and water subsampling. (bottom) Timeline of sample collection from the incubation chambers (blue = dissolved organic carbon [DOC] concentration and optical property aliquots; red = as blue, but with ^{14}C samples for DOC and CO_2). At day 138, three replicate samples were collected for $DO^{14}C$ and $^{14}CO_2$; at day 140, three replicate samples were collected for $PO^{14}C$.

(Dinsmore et al., 2010). This is an ombrotrophic peatland (85% of the catchment is peat), drained by a narrow open stream channel 0.7 m wide on average. Mean air temperature was 3.1 °C, total rainfall was 102 mm, and mean discharge in the Black Burn was 41 L/s for the month prior to sampling, with no unusual hydrological or climatic events for this time of year (Dinsmore et al., 2013; Pickard et al., 2017).

The aquatic C flux is dominated by DOC, with an annual yield of 19.3 ± 4.6 g $C{\cdot}m^{-2}{\cdot}year^{-1}$. CO_2 evasion is the second biggest component of aquatic C flux in the study catchment (10.0 g $C{\cdot}m^{-2}{\cdot}year^{-1}$; range = 2.33–24.0 g $C{\cdot}m^{-2}{\cdot}year^{-1}$). Other greenhouse gas fluxes are negligible compared with DOC export and CO_2 evasion (Dinsmore et al., 2013). Peat between 0.5 and 5 m thick overlies an extensive layer of glacial-derived boulder clay, which means that the underlying bedrock (predominantly Upper Carboniferous/Lower Devonian sandstones with occasional thin bands of limestone, mudstone, and coal) is likely less important to stream CO_2 fluxes compared with deep peat layers (Billett et al., 2007). Peat soils in the riparian zone of the Black Burn have provided ^{14}C ages of up to 1,400 years BP (83.93 pmC) at 70-cm depth (dates for deeper layers are not available but are likely older; Leith et al., 2014).

We prefiltered 60 L of stream water through a coarse nylon mesh (~225 μm) and homogenized it across two prerinsed 30-L barrels. The samples were collected at 3.7 °C (water temperature) and kept at that temperature and in the dark until the start of the incubation. Field parameters (pH, electrical conductivity [EC], and temperature) were measured at the site using a Hach PH101C pH probe and a CDC401 conductivity probe connected to an HQd portable meter; these measurements were repeated for the sample waters at the end of the incubation. Dissolved CO_2 (Hope et al., 1995) and DOC concentrations, and initial (t_0) measurements of $DO^{14}C$ and $^{14}CO_2$, were also collected in the field. The $DO^{14}C$ sample was collected in a 1-L acid-washed bottle and filtered to 0.7 μm on preashed (~500 °C for ~3 hr) Whatman glass fiber filters (GF/F) in the laboratory. The $^{14}CO_2$ sample was collected using the super-headspace method (see supporting information), collecting 3.5-ml CO_2 on a molecular sieve cartridge (Garnett, Billett, et al., 2016).

2.2. Incubations

The 60-L DOC-rich water sample was refrigerated at the University of Stirling overnight after sampling and thoroughly mixed and filtered the following day through preashed 0.7-μm GF/F filters at low pressure. This

filter size isolates the DOC size fraction but allows sufficient bacteria (both heterotrophic and autotrophic) to pass through the filter for incubation (Dean, van Hal, et al., 2018). Fourteen liters of filtrate was then transferred into each of the three replicate incubation chambers. The filled chambers were refrigerated until the incubations commenced on 19 March. Three water aliquots were collected during filtration to confirm the homogeneity of the incubation water (Table S1).

Incubation chambers were 17-L white high-density polyethylene (HDPE) barrels (Ampulla UK), UN Class 1 approved for storage of pharmaceuticals and food products (Figure 3). The chambers were cleaned with dilute Decon90 and thoroughly rinsed with distilled water prior to the experiment. We conducted blank test incubations using MilliQ®-grade deionized water in the same-class HDPE barrels to account for potential leaching from the incubation vessels. After 1 month, blank water samples contained 0.006 mg C/L, equivalent to <0.05% of the sample DOC content (Table S2). After 101 days, the blank water contained 0.01 mg C/L, approximately 0.1% of the sample DOC content (blank samples were processed in the same way as the DO^{14}C samples, but insufficient material was obtained to measure either δ^{13}C or ^{14}C content; see section 2.3). This shows that potential leaching from the HDPE incubation chambers used in this experiment was negligible and would not have impacted the ^{14}C results or DOC concentrations.

When filled with sample water, chambers had a 3-L headspace that was continuously flushed at a rate of approximately 150 cm^3/min (replacing the headspace in ~20 min) with outdoor ambient air scrubbed of CO_2 using an "indicating" soda lime trap (26-cm^3 volume) and Mg $(ClO_4)_2$ moisture trap via Tygon® medical-grade E-3606 tubing and mounted CPC couplings (Colder Products Co., USA) and then sealed with plastic paint (Plasti Dip, USA; Figure 3). The soda lime trap was replaced approximately halfway through the experiment, remaining fully functional for the duration of the experiment. Unfortunately, we were not able to monitor CO_2 concentrations in the system except during sampling.

A 140-mm-diameter circular hole was drilled into the lid of each chamber and covered with a 150-mm-diameter quartz glass window that allowed all wavelengths of light to pass through while preventing gas diffusion and then sealed with silicone sealant (Figure 3). The quartz glass window allowed both primary production and photo-oxidation to take place in the incubation chambers (see below). The chambers were equally irradiated with a T5 UV-B lamp (Arcadia Reptile, UK) designed to emit the full spectrum of natural light. The irradiance value measured on the sample surface was 14.5 W/m^2 (3.19 W/m^2 between 300 and 400 nm)—this is approximately twice the typical irradiance of the site where the incubation sample was collected, but the aim of the experimental design was to allow both autotrophic and heterotrophic DOC decomposition rather than specifically focus on either decomposition process. A night/day regime was used with a 12-hr equal split (8 a.m. to 8 p.m. light).

The incubated water was recirculated continuously using an external 12-V water pump at a rate of 15 ml/s, turning over the full water volume in 16 hr via mounted CPC couplings and E-3606 tubing, in order to replicate in-stream physical processes and limit stratification and heterogeneous mixing of solutes (Figure 3). The incubation system was designed to limit the ingress of ambient CO_2 by sealing the chambers and flushing the headspace with CO_2-free outside air (flushing was not possible during CO_2 sampling, which took between 40 and 170 min). Any ingress of ambient air that did occur during CO_2 sampling was corrected for using an established methodology for field-based chamber sampling (Gaudinski et al., 2000; Walker et al., 2016). Briefly, two δ^{13}C isotopic end-members, ambient lab air (Bilzon et al., 2002) and the oldest CO_2 sample collected, were used to estimate the relative contributions of each end-member to a given sample. This is then compared with our estimate of ambient air ingress into each sample based on measurements of air ingress rates into the chambers (see Supplementary Methods; Figure S2). The mixing of the incubated sample water and the regular supply of oxygen to the headspace meant that any CH_4 production was minimized. The incubations were started on 19 March 2015 and stopped on 6 August 2015. The experiment ran for 140 days to simulate longer potential residence times for DOC during aquatic transfer from the terrestrial to marine zone. While the half-life of OC within inland water systems is 2.5 ± 4.5 years (Catalán et al., 2016), average residence times in peatland streams could be much lower than this. But with drain blocking becoming an increasingly common peatland restoration technique (Evans et al., 2018), and peatlands providing a substantial proportion of water supply to reservoirs (Xu et al., 2018), residence times in the order of 140 days or longer are possible for peatland DOC within inland water systems.

2.3. Sample Collection and Analysis

Incubation aliquots for $DO^{14}C$ and $^{14}CO_2$ were collected from one chamber only (C2) on days 4 (t_1), 8 (t_2), 14 (t_3), 32 (t_4), 76 (t_5), and 138 (t_6; Figure 3). These were spread based on expected higher rates of DOC decomposition over the initial incubation period (Vonk et al., 2015). At the final time point, ^{14}C samples were collected from all three chambers. Incubation water aliquots were collected from each chamber via an outlet on the water pump line; headspace $^{14}CO_2$ samples were collected via the upper mounted CPC couplings (Figure 3). $DO^{14}C$ samples were collected in 500-ml acid-washed clear HDPE bottles after prerinsing with sample water, filtered to 0.7 μm on preashed GF/F filters and refrigerated until analysis (less than 90 days in all cases, which should not have impacted the stable or radiogenic isotopic signatures of the DOC sample; Gulliver et al., 2010). $^{14}CO_2$ samples were collected by first purging the headspace of CO_2 by cycling it through a soda lime CO_2 trap until the concentration was <60 ppm. The headspace was then allowed to equilibrate with the water by diffusion for 1 to 2 hr (overnight in one case; see Supplementary Methods). The headspace was then cycled through a molecular sieve trap to capture the CO_2 for ^{14}C analysis (1.5- to 4.1-ml CO_2; Table S1). Where insufficient sample was captured on the molecular sieve in one cycle, the headspace was then allowed to build up again for another 1 to 2 hr and sampled again.

Incubation aliquots for DOC concentrations (DOC and total C) and optical properties (absorbance and fluorescence) were collected in 30-ml sterile HDPE tubes (first rinsed with sample) during preincubation filtration and on days 1, 4, 7, 8, 14, 32, 34, 48, 62, 76, 97, 124, 138, and 140 (Figure 3). Dissolved organic matter (DOM—contains the DOC pool) quality parameters from absorbance and fluorescence measurements provide insights into the structure and molecular weight of the DOC pool (Fellman et al., 2010; Helms et al., 2008). Absorbance aliquots (50 mL) from the three replicate chambers were collected in sterile containers and then filtered through precombusted 0.7-μm Whatman GF/F filters under low pressure. Absorbance measurements were carried out immediately after sample collection using a dual-beam spectrophotometer (Agilent Cary 100; see Supplementary Methods). From the absorbance values, we calculated the ratio of the absorption spectral slopes between 275–295 and 350–400 nm (slope ratio, S_R), which is inversely correlated with DOM molecular weight (Fichot & Benner, 2012; Helms et al., 2008). Aliquots for the measurement of DOM fluorescence were only collected from chamber C2. DOM fluorescence was measured with a spectrofluorometer (Instant Screener®, Laser Diagnostic Instruments AS; see Supplementary Methods; Lawaetz & Stedmon, 2009; Murphy et al., 2010; Patel-Sorrentino, 2002) and used to calculate the humification index (HIX; the extent of humification in the DOM—i.e., how decomposed it is) by dividing the area under the emission spectra 435–480 nm by the peak area 300–345 nm + 435–480 nm, at excitation 254 nm (Ohno, 2002). Lower HIX values indicate more decomposition (increased humification) of the DOM pool. DOC quality and concentration aliquots collected before day 32 were not filtered prior to analysis. From day 34 onward, minor flocculation was first observed, so these samples were then filtered through 0.7-μm preashed GF/F filters, with negligible difference seen between days 32 and 34 (±1.0 mg C/L). DOC concentrations were measured at the University of Stirling on a Shimadzu Total Organic Carbon Analyzer (TOC-V series) with a lower detection limit of 0.5 μg/L and an accuracy of 1.5%.

POC concentration and ^{14}C samples were collected on day 140 only, by first stirring to homogenize the sample thoroughly, then filtering through 0.7-μm preashed GF/F filters, and measuring the captured material. One liter of sample water was filtered to obtain the $PO^{14}C$ samples, and 200 ml of water was filtered for triplicate particulate organic matter concentrations; the filters were then dried at 70 °C. POC concentration samples were combusted in a Carlo-Erba EA 1108 elemental analyzer, using sulfanilamide as the standard.

^{14}C samples were prepared for analysis at the Natural Environment Research Council Radiocarbon Facility (East Kilbride, UK). $DO^{14}C$ samples were processed to solids using rotary evaporation and then acid-fumigated (Dean, van der Velde, et al., 2018). $DO^{14}C$ and $PO^{14}C$ samples were combusted, and the CO_2 produced was cryogenically recovered. Molecular sieve cartridges were heated, and the desorbed sample CO_2 was cryogenically recovered (Garnett & Murray, 2013). For all ^{14}C samples, an aliquot of the recovered CO_2 was analyzed for $\delta^{13}C$ using isotope-ratio mass spectrometry (Thermo Fisher Delta V), with results reported relative to the Vienna Pee Dee Belemnite standard. A further aliquot of CO_2 was graphitized using Fe-Zn reduction and the ^{14}C content determined by accelerator mass spectrometry (AMS) at the Scottish Universities Environmental Research Centre (Xu et al., 2004). Following convention, all ^{14}C results were normalized using the $\delta^{13}C$ values and presented as pmC and conventional radiocarbon ages (years BP,

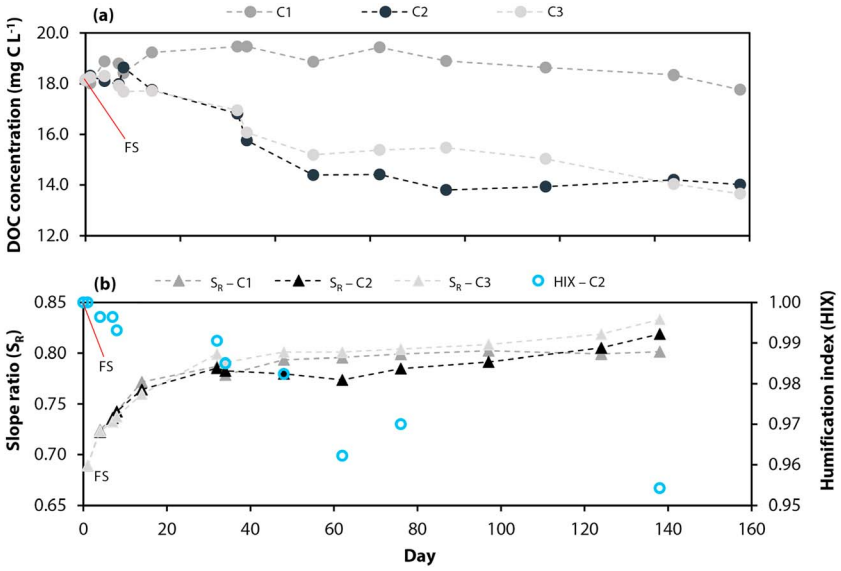

Figure 4. (a) Dissolved organic carbon (DOC) concentrations in each chamber (C1 = gray circles, C2 = black circles, C3 = light gray circles) during the 140-day incubation; (b) DOC structural proxies (slope ratio [S_R] = triangles, color coding as in Figure 4a; humification index [HIX] = blue hollow circles) during the incubation; "FS" denotes field samples. HIX values are only available for chamber C2 where the primary ^{14}C samples were collected from.

where 0 year BP is 1950 CE). The ^{14}C background associated with these methods was quantified by analysis of ^{14}C-dead materials (blanks); standards of known ^{14}C content processed alongside the samples gave values within 1σ of the consensus.

3. Results

3.1. Field Results

DOC and dissolved CO_2 concentrations at the field site were 18.4 ± 0.6 (Figure 4) and 2.3 ± 0.1 mg C/L, respectively, while pH was 5.9 and EC was 60.3 μS/cm. These values are usual for this time of year at the study site (Dinsmore et al., 2013), with average values in the 3 months prior to sampling being 5.1 for pH and 59.1 μS/cm for EC (Pickard et al., 2017). $DO^{14}C$ was 103.79 ± 0.48 pmC (i.e., modern; Figure 5), while $^{14}CO_2$ was 88.14 ± 0.38 pmC (1,014 ± 35 years BP; Figure 5). The ^{14}C results agree with previous work at the site and similar temperate peatlands where DOC was modern, while CO_2 was consistently older (Billett et al., 2007; Billett & Garnett, 2010; Leith et al., 2014).

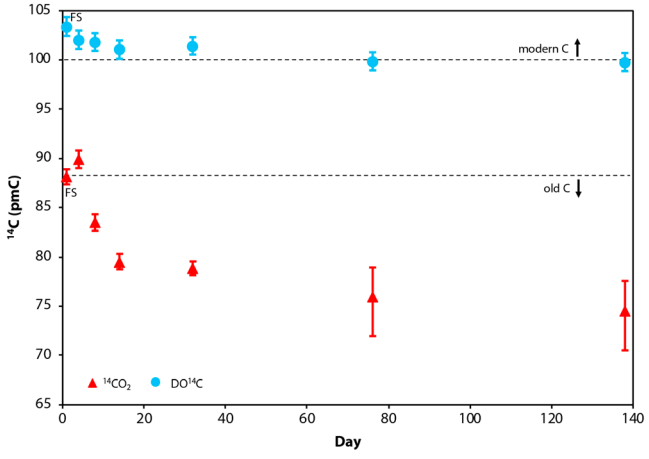

Figure 5. ^{14}C of CO_2 (red triangles) and dissolved organic carbon (blue circles) in chamber C2 over the course of the incubation; uncertainty ranges for $DO^{14}C$ are 2σ analytical error; uncertainty ranges for $^{14}CO_2$ are derived from the correction for atmospheric ingress (see Supplementary Methods). "FS" denotes field samples; modern C (>100 percent modern C [pmC]) and old C (>1,000 years BP) age ranges are indicated by the dashed horizontal lines.

3.2. DOC Decomposition and ^{14}C Dynamics

$DO^{14}C$ content decreased from 102.45 ± 0.47 pmC (modern) at t_1, very similar to the field sample, to 99.78 ± 0.46 pmC (17 ± 17 years BP) over 138 days of incubation (Figure 5). $\delta^{13}C$-DOC changed only slightly, from −28.7‰ to −28.2‰ during incubation (Table 1). The final $DO^{14}C$ concentration was consistent across all three chambers with a range of 99.16 ± 0.45 to 99.83 ± 0.44 pmC. While the reduction in $DO^{14}C$ content over the 138 days of incubation was relatively small (Table 1 and Figure 5), it is statistically significant ($p < 0.05$ for the three t_6 samples; Student's t test, R version 3.4.3) and implies a small shift toward older DOC.

DOC concentrations in chambers C2 (where the primary ^{14}C measurements were collected) and C3 behaved similarly, remaining relatively stable for the first 8 to 14 days at a maximum of 18.6 mg C/L, before

Table 1
The ^{14}C and $\delta^{13}C$ Data for DOC, POC, and CO_2 From the Incubation and Field Samples Collected in This Study

		DO^{14}C		δ^{13}C-DOC	$^{14}CO_2$		$\delta^{13}CO_2$	PO^{14}C[a]		δ^{13}C-POC[a]
Day	Location	pmC ± 1σ	Age (years BP)	‰ (±0.1)	pmC ± 1σ	Age (years BP)	‰ (±0.1)	pmC ± 1σ	Age (years BP)	‰ (±0.1)
0	Field	103.79 ± 0.48	Modern	−28.8	88.14 ± 0.38	1,014 ± 35	−18.6	—	—	—
4	Chamber 2	102.05 ± 0.47	Modern	−28.7	89.92 ± 0.90[b]	853 ± 100[b]	[b]	—	—	—
8	Chamber 2	101.82 ± 0.45	Modern	−28.5	83.50 ± 0.83[b]	1,448 ± 53[b]	[b]	—	—	—
14	Chamber 2	101.05 ± 0.47	Modern	−28.6	79.54 ± 0.79[b]	1,838 ± 97[b]	[b]	—	—	—
32	Chamber 2	101.43 ± 0.44	Modern	−28.5	78.91 ± 0.35	1,903 ± 36	−27.1	—	—	—
76	Chamber 2	99.86 ± 0.46	11 ± 37	−28.5	76.01 ± 3.49[b]	2,204 ± 744[b]	[b]	—	—	—
138	Chamber 1	99.16 ± 0.45	69 ± 37	−28.6	80.47 ± 0.84[b]	1,746 ± 124[b]	[b]	77.05 ± 0.35	2,094 ± 37	−32.3
138	Chamber 2	99.78 ± 0.46	17 ± 17	−28.2	74.58 ± 3.53[b]	2,356 ± 767[b]	[b]	77.70 ± 0.36	2,027 ± 37	−30.6
138	Chamber 3	99.83 ± 0.44	14 ± 14	−28.4	83.60 ± 1.45[b]	1,439 ± 280[b]	[b]	79.68 ± 0.37	1,824 ± 37	−30.5

Note. pmC = percent modern C; years BP = years before present (where 0 year BP = 1950 CE); DOC = dissolved organic carbon; POC = particulate organic carbon.
[a]POC samples collected on day 140. [b]CO_2 isotopic values corrected for atmospheric contamination, and the uncertainty from this correction (95% confidence interval) is included in the uncertainties here (see Table S3 for uncorrected values).

declining from day 14 to day 138, reaching a low of 13.7 mg/L (Figure 4a). DOC in chamber C1, however, increased in concentration until day 34 (19.46 mg/L) and then declined gradually to 17.8 mg/L at day 138 (Figure 4a).

S_R increased across all chambers, indicating a decline in molecular weight that suggests larger DOM molecules were continually broken down over the course of the incubation (Figure 4b). The increase in S_R was reflected in a 28.7–35.7% reduction in the absorption coefficient at 254 nm, a 31.8–40.2% reduction at 300 nm, and a 30.9–44.9% reduction at 440 nm, suggesting an overall decline in aromaticity and molecular weight (Table S1). HIX values, calculated from the DOM fluorescence measurements from chamber C2, decreased from >0.99 (measurement saturated) to 0.95, indicating a reduction in humic substances in the DOC pool (Figure 4b).

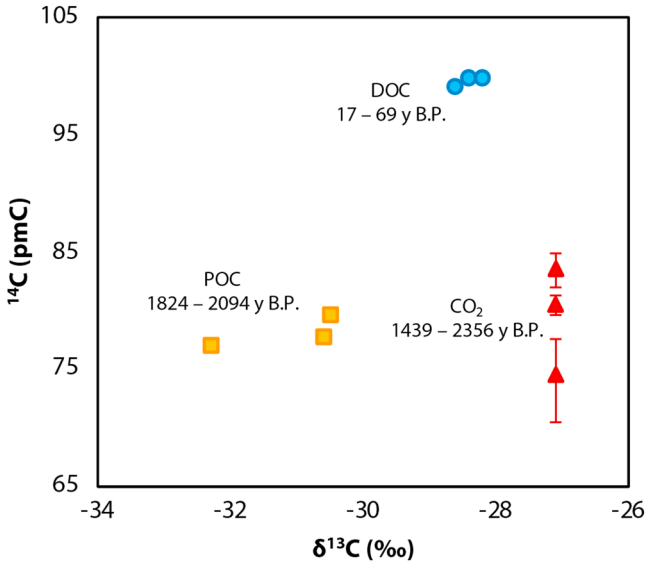

Figure 6. The relationship between ^{14}C and $\delta^{13}C$ for the dissolved organic carbon (DOC; blue circles), particulate organic carbon (POC; orange squares), and CO_2 (red triangles) pools from the final time point (140 days) for all chambers. The CO_2 (derived from the decomposition of the DOC pool) and the POC (derived from microbial growth and flocculation) are both significantly older (less ^{14}C enriched) than the DOC. The uncertainty ranges for DOC and POC are derived from the analytical uncertainty and are smaller than the symbols shown in the figure; CO_2 uncertainty ranges are derived from the correction for atmospheric ingress (see Supplementary Methods).

3.3. $^{14}CO_2$ dynamics

During the incubation, headspace $^{14}CO_2$ signatures fell from 89.92 ± 0.90 pmC (853 ± 100 years BP) at t_1 to 74.58 ± 3.53 (2,356 ± 767 years BP) at the final time point (Figure 5). The t_1 $^{14}CO_2$ age was slightly younger than the field $^{14}CO_2$ sample, indicating that, initially, younger DOC was decomposing to produce CO_2. The subsequent increase in $^{14}CO_2$ age was supported by replicate ^{14}C measurements at the final time point in chambers 1 and 3 of 80.47 ± 0.84 and 83.60 ± 1.45 pmC (1,746 ± 124 and 1,439 ± 280 years BP, respectively; Table 1 and Figure 6). The pH and EC of the incubated water remained stable at 5.8–5.9 and 59.8–63.7, respectively, indicating that dissolved inorganic C was predominantly present as dissolved CO_2, which would be in isotopic equilibrium with the sampled headspace CO_2.

The $\delta^{13}C$ values can also indicate CO_2 source, alongside ^{14}C. The field CO_2 sample had a $\delta^{13}C$ signature of −18.6 ‰, which was higher than the CO_2 produced directly from the decomposition of the DOC pool (−27.1 ‰; Table 1). The field $\delta^{13}CO_2$ value was matched by an old ^{14}C age, suggesting it was sourced in part by the decomposition of deep peat layers (Billett et al., 2007; Dean, van der Velde, et al., 2018) and potentially $^{13}CO_2$ fractionation during evasion from the stream (Doctor et al., 2008). The lower $\delta^{13}CO_2$ value from the incubation matches that of DOC (−28.4‰ to −28.8‰; Table 1), supporting the case for the old $^{14}CO_2$ ages measured during the incubation being directly produced from the decomposition of the DOC pool.

3.4. The Production of CO_2 and POC From Decomposition of the DOC Pool

POC was formed in the incubation chambers during the experiment, and this also had an old ^{14}C signature of 1,824 ± 37 to 2,094 ± 37 years BP (Table 1 and Figure 6). This POC formed from large-scale microbial growth, driven by heterotrophic and autotrophic production, causing flocculation of living and dead microbial biomass and OC, and the formation of microbial biofilms (Figure S2; Battin et al., 2016; Logue et al., 2016). POC was not present at the beginning of the incubation as we filtered the sample water to isolate the DOC pool.

Isotope mass balance equations can be useful for partitioning C sources (Billett et al., 2007). During the incubation, old C was predominantly partitioned into the CO_2 and POC pools (Figure 6). To satisfy isotope mass balance, the DOC age would be expected to remain constant or become younger (more ^{14}C enriched) as old C was lost to CO_2 and POC. For example, we used equation (1) to estimate the ^{14}C content of the DOC pool that was lost during the course of the incubation:

$$\Delta_{\text{lost}} \times M_{\text{lost}} = \Delta_{t0} \times M_{t0} - \Delta_{t6} \times M_{t6} \quad (1)$$

where Δ represent the ^{14}C content (pmC) and M the mass of the DOC lost during the incubation ($_{\text{lost}}$) and at the start ($_{t0}$) and end ($_{t6}$) of the incubation. Because the age of DOC increased over time (i.e., ^{14}C depleted; Figure 5), equation (1) predicts the ^{14}C content of the CO_2 produced from the decomposition of the DOC pool to be ^{14}C enriched (117.6 pmC). However, this value contrasts with our direct observations of the predominantly old C in the CO_2 and POC pools (Figure 6).

4. Discussion

4.1. Carbon (Re)Cycling in the Incubation Chambers

The observed increase in DOC age in conjunction with the production of old CO_2 and POC pools during the experiment could be explained by the rapid loss of a modern component of the DOC pool early in the incubation and the reintroduction of old C into the DOC pool by autotrophic fixation. If there was rapid respiration of a labile modern component of the DOC pool (e.g., plant exudates and leachates from freshly decayed organic matter), then the resultant CO_2 could have been flushed from the headspace and thus missed in the first days of the incubation (the chambers were not closed systems). This is hinted at by the t_1 CO_2, which was generated directly from the decomposition of the DOC pool, being younger than the field CO_2, which was an integrated CO_2 pool generated from the decomposition of OC throughout the catchment peat soil profiles as well as within the stream itself (Figure 5). As this labile modern DOC pool rapidly decomposed over the early phase of the incubation and was flushed from the headspace, the old C signature would have become more pronounced in the respired CO_2, which can be seen in Figure 5. An additional mechanism, the growth of autotrophic microorganisms, would have fixed free (dissolved) CO_2 into the microbial-DOC pool through photosynthesis. This mechanism can at least partially explain the partitioning of C ages in the incubation systems. The free CO_2 in the incubation system may have been younger, initially, as described above, but rapidly aged between t_1 and t_2 (4 days; Figure 5), yielding old CO_2 for subsequent autotrophic fixation and incorporation into autotrophic biomass and POC formation. Microbial biomass and detritus less than 0.7 μm in size are also considered part of the DOC pool and are included in the $DO^{14}C$ and DOC concentration measurements for this experiment, so the reintroduction of old C in the DOC pool could also explain the increase in the bulk $DO^{14}C$ age (Fellman et al., 2010).

4.2. The Potential Hidden Age of Peatland Stream DOC

Our study supports the hypothesis that peatland stream DOC with a modern age can contain a fraction of old C that is available for decomposition during aquatic transport. Old C was identified in the CO_2 produced from the decomposition of the predominantly modern DOC pool within 20 days (Figure 5), well within the half-life of OC within inland water systems (2.5 ± 4.5 years; Catalán et al., 2016). The increase in DOC concentrations observed in chamber C1 may have been due to increased autotrophic microbial growth in this chamber compared with the others (some microbial biomass is incorporated into DOC; see section 3.4). However, shifts in DOM structure across all three incubation chambers show that the terrestrial DOC pool was continually being decomposed for the duration of the experiment, despite DOC dynamics being influenced by autotrophic and heterotrophic microbial growth, (Figure 4 and Table S1). The observed

decline in HIX values (Figure 4) is likely due to the preferential decomposition of terrestrial-derived (humic) DOC, rather than the decomposition of heterotrophic and autotrophic microbial biomass that also contributes to the overall DOC pool (Fellman et al., 2010). The terrestrial-derived component of the DOC pool is likely old (Galy & Eglinton, 2011; Leith et al., 2014), and the HIX dynamics suggest that this old terrestrial OC was continually decomposed over the incubation, fueling CO_2 production as reflected in the old $^{14}CO_2$ signature we observe (Figure 5). DOM structural shifts were consistent across all the incubation chambers (Figure 4b), suggesting that although the kinetics of DOC decomposition in chamber C1 may have been different from the others, the overall decomposition of the DOC pool and ^{14}C results are comparable across all chambers (Figure 6). However, fluxes of CO_2 produced in the different chambers were not measured to corroborate this.

There was an increase in the difference between the incubation $DO^{14}C$ and $^{14}CO_2$ signatures as the experiment progressed. This difference rapidly increased over the first 14 days and then plateaued (Figure 5). This is consistent with the rapid respiration of a labile modern component of the DOC pool and increased decomposition of old C once this labile modern pool was lost. Previous work also demonstrated the likely presence of a labile young C component with bulk riverine DOC loads (Galy & Eglinton, 2011; Loh et al., 2006; Raymond & Bauer, 2001). We were not able to quantify the amount of modern labile C that was rapidly lost in the initial stages of the incubation. But this fraction cannot have been the majority of the modern DOC component because the bulk $DO^{14}C$ signature remained close to modern for the duration of the experiment. This indicates that there was a substantial recalcitrant modern DOC component. In this experiment, we clearly demonstrate that there is also potential for an important component of labile old C to be hidden within bulk "modern" riverine DOC loads. This old C signal may have been exaggerated in our experimental system due to the rapid respiration and flushing from the system of a labile modern DOC component and the later reintroduction of C into autotrophic biomass (see section 3.4). However, that the presence of old C is observed at all, and at such clear levels in the CO_2 and POC measurements, unequivocally supports our hypothesis that labile old C can be concealed within bulk modern DOC pools.

Previous work has shown that heterotrophic respiration of temperate lake DOC produced old CO_2 (1,000 to 3,000 years BP) despite the bulk ^{14}C signature of the incubated DOC being significantly younger (modern, with ^{14}C contents of 101.4 to 111.0 pmC; McCallister & del Giorgio, 2012). The degradation of ancient C (>11,300 years BP) has also been demonstrated in Arctic yedoma permafrost (Drake et al., 2015; Mann et al., 2015; Spencer et al., 2015; Vonk et al., 2013). In contrast, earlier work suggests that modern C is preferentially respired from bulk riverine DOC loads, with old C remaining recalcitrant (Galy & Eglinton, 2011; Raymond & Bauer, 2001). However, concurrent in situ measurements of aquatic $DO^{14}C$ and $^{14}CO_2$ signatures are rare, limited to four studies, of which we are aware. Aquatic CO_2 is generally older than DOC in UK peatlands, including the study site where we collected our DOC sample for incubation (Billett et al., 2007, 2012; Leith et al., 2014). This was thought to be driven by a mixed signal comprising ^{14}C-dead CO_2 from geological sources (~5–30%) and modern CO_2 derived from soil respiration in the upper peat layers (~70–95%). DOC was older than CO_2 in a western Canadian Arctic peatland underlain by continuous permafrost (Dean, van der Velde, et al., 2018). There, the shallow permafrost prevented contributions of ^{14}C-dead geogenic sources, with the CO_2 and DOC sourced from both old and young shallow peat layers. The results of the incubation study presented here, where external C inputs to the $^{14}CO_2$ signal are restricted, suggest that respiration of old C within bulk DOC pool also contributes to in situ riverine $^{14}CO_2$ signals. However, this is highly system dependent, with different DOC age components available for decomposition to CO_2 during aquatic transport and storage.

4.3. Implications and Future Work

Bulk $DO^{14}C$ measurements are not sensitive enough to detect old C in peatland inland water systems, as demonstrated by the production of old $^{14}CO_2$ from the decomposition of a bulk modern $DO^{14}C$ sample in the experiment presented here—with the exception of severe cases of landscape disturbance (Figure 1). The findings of this study also suggest that bulk $DO^{14}C$ measurements do not represent the ^{14}C signature of the labile OC pool exported by inland water systems more broadly (Fellman et al., 2014). In situ aquatic $^{14}CO_2$ measurements in UK peatlands were previously thought to show a mixture of modern soil and ^{14}C-dead geological sources (Billett et al., 2007). This experiment suggests that there is also a component of old C that remains recalcitrant in oxygen-poor peat layers for many thousands of years but becomes

available for decomposition after its release by variable mixing with water flowing through the peat soil layers (Dean, van der Velde, et al., 2018; van der Velde et al., 2012). This shift from recalcitrant to labile may be driven by the change from oxygen-poor to oxygen-rich conditions, differing microbial populations in the aquatic zone from the soil zone (Dean, van Hal, et al., 2018), and/or combined photodecomposition and microbial decomposition. All of these processes were operating in the experiment presented here (Figure 3). However, we did not separate them out by experimental design, seeking only to simulate natural in-stream conditions for a single site. Further studies should be carried out to distinguish the importance of these individual processes to DOC lability during transport and storage in inland water systems and across a range of ecosystems.

These findings may extend beyond aquatic respiration and may be relevant to the interpretation of ^{14}C studies on soil respiration and porewater $DO^{14}C$. Further, other aquatic C species may also be affected by components of differing C age and lability. Incubations such as the one presented here can aid this research strand, although they require multiple ^{14}C dates and are time-consuming. For bulk POC and DOC samples, ramped pyrolysis can reveal the ^{14}C signature of C combusted at different temperatures (i.e., indicating lability; e.g., Zhang et al., 2017), although this has only recently been developed for bulk aquatic DOC samples (Hemingway et al., 2017). Matching ramped pyrolysis $DO^{14}C$ signatures and integrated soil OC age distributions (Sierra et al., 2017) with bulk $DO^{14}C$ samples via age distribution models (e.g., Figure 2) would improve our estimates of the likely proportions of different aged C within bulk $DO^{14}C$ samples (Evans et al., 2014). This could be assisted by compound-specific ^{14}C methods (e.g., Feng et al., 2013, 2017), although this can also require multiple ^{14}C dates for a single sample depending on the target organic compounds, and it is possible that C of multiple ages can be present within the isolated pools.

Direct in situ measurements of $^{14}CO_2$ and $^{14}CH_4$ signatures are needed to improve our understanding of the contribution of old C to inland water C emissions across a range of environmental settings. Methodological advances now allow for the collection of $^{14}CO_2$ and $^{14}CH_4$ samples relatively quickly and easily in even remote field locations (Billett et al., 2006; Dean et al., 2017; Garnett, Billett, et al., 2016; Garnett, Gulliver, et al., 2016). For aquatic CO_2 and CH_4 ^{14}C samples, age distribution analysis (e.g., Dean, van der Velde, et al., 2018) or multisource isotopic mass balance (e.g., Elder et al., 2018) can help determine relative contributions of different aged C.

Acknowledgments
We thank the staff at the NERC Radiocarbon Facility (NRCF010001) and the SUERC AMS Laboratory. We are grateful to Prof. Jesus Torres Palenzuela of University of Vigo for the fluorescence measurements; to Ian Washbourne and Kerry Dinsmore at the Centre for Ecology and Hydrology, Penicuik, UK, for the field CO_2 and CH_4 concentration analyses; and to Ype van der Velde at Vrije Universiteit Amsterdam for his assistance with the age distribution calculations. We also thank two anonymous reviewers and the Editor for their constructive comments that substantially improved this paper. This work was supported by the NERC Radiocarbon Facility NRCF010001 (allocation number 1855.1014). J. F. D. received partial support from the program of the Netherlands Earth System Science Centre (NESSC), financially supported by the Ministry of Education, Culture and Science (OCW) (grant number 024.002.001). The data supporting these conclusions are all included within the paper itself or the supporting information accompanying it. Any requests for further information or data should be directed to J. F. D. The authors declare no competing financial interest.

5. Conclusions

In the incubation experiment presented here, old C up to 2,350 years BP was clearly identified in the CO_2 produced from the decomposition of a bulk "modern" DOC pool. Bulk ^{14}C dating of peatland stream DOC may therefore be an insensitive environmental indicator for the export of old riverine C. Consideration should be given to collecting a suite of ^{14}C measurements (e.g., $PO^{14}C$, $^{14}CO_2$, and $^{14}CH_4$) to complement $DO^{14}C$ analyses and obtain an accurate representation of the age of mobile OC within fluvial systems. Our study also suggests that old C may be an important contributor to CO_2 emissions from inland waters, which are a large source of C to the atmosphere. Understanding the proportion of old C released to the atmosphere within this flux is of great importance for modeling ecosystem productivity and C cycling and for predicting the impacts of future climate change at the global scale (Cole et al., 2007). This is especially true for peatlands, which are considered a key C sink in the global C cycle (Billett et al., 2015). An increased proportion of old C in riverine DOC export means a potential increase in old C lost to the atmosphere and delivered to the oceans (Battin et al., 2009; Bogard & Butman, 2018). This suggests that there may be more old C involved in the global C cycle than previously thought (Butman et al., 2015; Fellman et al., 2014; Guillemette et al., 2017).

References

Aiken, G. R., Spencer, R. G. M., Striegl, R. G., Schuster, P. F., & Raymond, P. A. (2014). Influences of glacier melt and permafrost thaw on the age of dissolved organic carbon in the Yukon River basin. *Global Biogeochemical Cycles*, *28*, 525–537. https://doi.org/10.1002/2013GB004764

Battin, T. J., Besemer, K., Bengtsson, M. M., Romani, A. M., & Packmann, A. I. (2016). The ecology and biogeochemistry of stream biofilms. *Nature Reviews Microbiology*, *14*(4), 251–263. https://doi.org/10.1038/nrmicro.2016.15

Battin, T. J., Luyssaert, S., Kaplan, L. A., Aufdenkampe, A. K., Richter, A., & Tranvik, L. J. (2009). The boundless carbon cycle. *Nature Geoscience*, *2*(9), 598–600. https://doi.org/10.1038/ngeo618

Billett, M. F., Charman, D. J., Clark, J. M., Evans, C. D., Evans, M. G., Ostle, N. J., Worrall, F., et al. (2010). Carbon balance of UK peatlands: Current state of knowledge and future research challenges. *Climate Research*, *45*(1), 13–29. https://doi.org/10.3354/cr00903

Billett, M. F., Dinsmore, K. J., Smart, R. P., Garnett, M. H., Holden, J., Chapman, P., Baird, A. J., et al. (2012). Variable source and age of different forms of carbon released from natural peatland pipes. *Journal of Geophysical Research*, *117*, G02003. https://doi.org/10.1029/2011JG001807

Billett, M. F., & Garnett, M. H. (2010). Isotopic composition of carbon dioxide lost by evasion from surface water to the atmosphere: Methodological comparison of a direct and indirect approach. *Limnology and Oceanography: Methods*, *8*, 45–53. https://doi.org/10.4319/lom.2010.8.0045

Billett, M. F., Garnett, M. H., & Dinsmore, K. J. (2015). Should aquatic CO_2 evasion be included in contemporary carbon budgets for peatland ecosystems? *Ecosystems*, *18*(3), 471–480. https://doi.org/10.1007/s10021-014-9838-5

Billett, M. F., Garnett, M. H., & Hardie, S. M. L. (2006). A direct method to measure $^{14}CO_2$ lost by evasion from surface waters. *Radiocarbon*, *48*(1), 61–68. https://doi.org/10.1017/S0033822200035396

Billett, M. F., Garnett, M. H., & Harvey, F. (2007). UK peatland streams release old carbon dioxide to the atmosphere and young dissolved organic carbon to rivers. *Geophysical Research Letters*, *34*, L23401. https://doi.org/10.1029/2007GL031797

Bilzon, J., Murphy, J., Allsopp, A., Wootton, S., & Williams, C. (2002). Influence of glucose ingestion by humans during recovery from exercise on substrate utilisation during subsequent exercise in a warm environment. *European Journal of Applied Physiology*, *87*(4–5), 318–326. https://doi.org/10.1007/s00421-002-0614-4

Bogard, M. J., & Butman, D. E. (2018). No blast from the past. *Nature Climate Change*, *8*(2), 99–100. https://doi.org/10.1038/s41558-018-0070-8

Butman, D. E., Wilson, H. F., Barnes, R. T., Xenopoulos, M. A., & Raymond, P. A. (2015). Increased mobilization of aged carbon to rivers by human disturbance. *Nature Geoscience*, *8*(2), 112–116. https://doi.org/10.1038/NGEO2322

Campeau, A., Bishop, K. H., Billett, M. F., Garnett, M. H., Laudon, H., Leach, J. A., et al. (2017). Aquatic export of young dissolved and gaseous carbon from a pristine boreal fen: Implications for peat carbon stock stability. *Global Change Biology*, *23*(12), 5523–5536. https://doi.org/10.1111/gcb.13815

Catalán, N., Marcé, R., Kothawala, D. N., & Tranvik, L. J. (2016). Organic carbon decomposition rates controlled by water retention time across inland waters. *Nature Geoscience*, *9*(7), 501–504. https://doi.org/10.1038/ngeo2720

Cole, J. J., Prairie, Y. T., Caraco, N. F., McDowell, W. H., Tranvik, L. J., Striegl, R. G., et al. (2007). Plumbing the global carbon cycle: Integrating inland waters into the terrestrial carbon budget. *Ecosystems*, *10*(1), 172–185. https://doi.org/10.1007/s10021-006-9013-8

Cory, R. M., & Kling, G. W. (2018). Interactions between sunlight and microorganisms influence dissolved organic matter degradation along the aquatic continuum. *Limnology and Oceanography Letters*, *3*(3), 102–116. https://doi.org/10.1002/lol2.10060

Dargie, G. C., Lewis, S. L., Lawson, I. T., Mitchard, E. T. A., Page, S. E., Bocko, Y. E., & Ifo, S. A. (2017). Age, extent and carbon storage of the central Congo Basin peatland complex. *Nature*, *542*(7639), 86–90. https://doi.org/10.1038/nature21048

Dawson, J. J. C., Bakewell, C., & Billett, M. F. (2001). Is in-stream processing an important control on spatial changes in carbon fluxes in headwater catchments? *Science of the Total Environment*, *265*(1-3), 153–167. https://doi.org/10.1016/S0048-9697(00)00656-2

Dean, J. F., Billett, M. F., Murray, C., & Garnett, M. H. (2017). Ancient dissolved methane in inland waters revealed by a new collection method at low field concentrations for radiocarbon (^{14}C) analysis. *Water Research*, *115*, 236–244. https://doi.org/10.1016/j.watres.2017.03.009

Dean, J. F., van Hal, J. R., Dolman, A. J., Aerts, R., & Weedon, J. T. (2018). Filtration artefacts in bacterial community composition can affect the outcome of dissolved organic matter biolability assays. *Biogeosciences*, *15*(23), 7141–7154. https://doi.org/10.5194/bg-15-7141-2018

Dean, J. F., van der Velde, Y., Garnett, M. H., Dinsmore, K. J., Baxter, R., Lessels, J. S., et al. (2018). Abundant pre-industrial carbon detected in Canadian Arctic headwaters: Implications for the permafrost carbon feedback. *Environmental Research Letters*, *13*(3), 034024. https://doi.org/10.1088/1748-9326/aaa1fe

van der Velde, Y., Torfs, P. J. J. F., van der Zee, S. E. A. T. M., & Uijlenhoet, R. (2012). Quantifying catchment-scale mixing and its effect on time-varying travel time distributions. *Water Resources Research*, *48*, W06536. https://doi.org/10.1029/2011WR011310

Dinsmore, K. J., Billett, M. F., & Dyson, K. E. (2013). Temperature and precipitation drive temporal variability in aquatic carbon and GHG concentrations and fluxes in a peatland catchment. *Global Change Biology*, *19*(7), 2133–2148. https://doi.org/10.1111/gcb.12209

Dinsmore, K. J., Billett, M. F., Skiba, U. M., Rees, R. M., Drewer, J., & Helfter, C. (2010). Role of the aquatic pathway in the carbon and greenhouse gas budgets of a peatland catchment. *Global Change Biology*, *16*(10), 2750–2762. https://doi.org/10.1111/j.1365-2486.2009.02119.x

Doctor, D. H., Kendall, C., Sebestyen, S. D., Shanley, J. B., Ohte, N., & Boyer, E. W. (2008). Carbon isotope fractionation of dissolved inorganic carbon (DIC) due to outgassing of carbon dioxide from a headwater stream. *Hydrological Processes*, *22*(14), 2410–2423. https://doi.org/10.1002/hyp.6833

Drake, T. W., Wickland, K. P., Spencer, R. G. M., McKnight, D. M., & Striegl, R. G. (2015). Ancient low-molecular-weight organic acids in permafrost fuel rapid carbon dioxide production upon thaw. *Proceedings of the National Academy of Sciences of the United States of America*, *112*(45), 13,946–13,951. https://doi.org/10.1073/pnas.1511705112

Dutta, K. (2016). Sun, ocean, nuclear bombs, and fossil fuels: Radiocarbon variations and implications for high-resolution dating. *Annual Review of Earth and Planetary Sciences*, *44*(1), 239–275. https://doi.org/10.1146/annurev-earth-060115-012333

Elder, C. D., Xu, X., Walker, J., Schnell, J. L., Hinkel, K. M., Townsend-Small, A., et al. (2018). Greenhouse gas emissions from diverse Arctic Alaskan lakes are dominated by young carbon. *Nature Climate Change*, *8*(2), 166–171. https://doi.org/10.1038/s41558-017-0066-9

Evans, C. D., Page, S. E., Jones, T., Moore, S., Gauci, V., Laiho, R., et al. (2014). Contrasting vulnerability of drained tropical and high-latitude peatlands to fluvial loss of stored carbon. *Global Biogeochemical Cycles*, *28*, 1215–1234. https://doi.org/10.1002/2013GB004782

Evans, C. D., Peacock, M., Green, S. M., Holden, J., Chapman, P. J., Lebron, I., et al. (2018). The impact of ditch blocking on fluvial carbon export from a UK blanket bog. *Hydrological Processes*, *32*(13), 2141–2154. https://doi.org/10.1002/hyp.13158

Fellman, J., Spencer, R. G. M., Raymond, P. A., Pettit, N. E., Skrzypek, G., Hernes, P. J., & Grierson, P. F. (2014). Dissolved organic carbon biolability decreases along with its modernization in fluvial networks in an ancient landscape. *Ecology*, *95*(9), 2622–2632. https://doi.org/10.1890/13-1360.1

Fellman, J. B., Hood, E., & Spencer, R. G. M. (2010). Fluorescence spectroscopy opens new windows into dissolved organic matter dynamics in freshwater ecosystems: A review. *Limnology and Oceanography*, *55*(6), 2452–2462. https://doi.org/10.4319/lo.2010.55.6.2452

Feng, X., Vonk, J. E., Griffin, C., Zimov, N., Montluçon, D. B., Wacker, L., & Eglinton, T. I. (2017). 14 C variation of dissolved lignin in Arctic river systems. *ACS Earth and Space Chemistry*, *1*(6), 334–344. https://doi.org/10.1021/acsearthspacechem.7b00055

Feng, X., Vonk, J. E., van Dongen, B. E., Gustafsson, Ö., Semiletov, I. P., Dudarev, O. V., et al. (2013). Differential mobilization of terrestrial carbon pools in Eurasian Arctic river basins. *Proceedings of the National Academy of Sciences of the United States of America*, *110*(35), 14,168–14,173. https://doi.org/10.1073/pnas.1307031110

Fichot, C. G., & Benner, R. (2012). The spectral slope coefficient of chromophoric dissolved organic matter (S275-295) as a tracer of terrigenous dissolved organic carbon in river-influenced ocean margins. *Limnology and Oceanography*, *57*(5), 1453–1466. https://doi.org/10.4319/lo.2012.57.5.1453

Galy, V., & Eglinton, T. (2011). Protracted storage of biospheric carbon in the Ganges–Brahmaputra basin. *Nature Geoscience*, *4*(12), 843–847. https://doi.org/10.1038/ngeo1293

Garnett, M. H., Billett, M. F. F., Gulliver, P., & Dean, J. F. (2016). A new field approach for the collection of samples for aquatic $^{14}CO_2$ analysis using headspace equilibration and molecular sieve traps: The super headspace method. *Ecohydrology*, *9*(8), 1630–1638. https://doi.org/10.1002/eco.1754

Garnett, M. H., Dinsmore, K. J., & Billett, M. F. (2012). Annual variability in the radiocarbon age and source of dissolved CO_2 in a peatland stream. *Science of the Total Environment*, *427-428*, 277–285. https://doi.org/10.1016/j.scitotenv.2012.03.087

Garnett, M. H., Gulliver, P., & Billett, M. F. (2016). A rapid method to collect methane from peatland streams for radiocarbon analysis. *Ecohydrology*, *9*(1), 113–121. https://doi.org/10.1002/eco.1617

Garnett, M. H., & Hardie, S. M. L. (2009). Isotope (^{14}C and ^{13}C) analysis of deep peat CO_2 using a passive sampling technique. *Soil Biology and Biochemistry*, *41*(12), 2477–2483. https://doi.org/10.1016/j.soilbio.2009.09.004

Garnett, M. H., Hardie, S. M. L., & Murray, C. (2011). Radiocarbon and stable carbon analysis of dissolved methane and carbon dioxide from the profile of a raised peat bog. *Radiocarbon*, *53*(01), 71–83. https://doi.org/10.1017/S0033822200034366

Garnett, M. H., Hardie, S. M. L., Murray, C., & Billett, M. F. (2013). Radiocarbon dating of methane and carbon dioxide evaded from a temperate peatland stream. *Biogeochemistry*, *114*(1–3), 213–223. https://doi.org/10.1007/s10533-012-9804-2

Garnett, M. H., & Murray, C. (2013). Processing of CO_2 samples collected using zeolite molecular sieve for ^{14}C analysis at the NERC Radiocarbon Facility (East Kilbride, UK). *Radiocarbon*, *55*(02), 410–415. https://doi.org/10.1017/S0033822200057532

Gaudinski, J. B., Trumbore, S. E., Davidson, E. A., & Zheng, S. (2000). Soil carbon cycling in a temperate forest: Radiocarbon-based estimates of residence times, sequestration rates and partitioning of fluxes. *Biogeochemistry*, *51*(1), 33–69. https://doi.org/10.1023/A:1006301010014

Guillemette, F., Bianchi, T. S., & Spencer, R. G. M. (2017). Old before your time: Ancient carbon incorporation in contemporary aquatic foodwebs. *Limnology and Oceanography*, *62*(4), 1682–1700. https://doi.org/10.1002/lno.10525

Gulliver, P., Waldron, S., Scott, E. M., & Bryant, C. L. (2010). The effect of storage on the radiocarbon, stable carbon and nitrogen isotopic signatures and concentrations of riverine DOM. *Radiocarbon*, *52*(03), 1113–1122. https://doi.org/10.1017/S0033822200046191

Helms, J. R., Stubbins, A., Ritchie, J. D., Minor, E. C., Kieber, D. J., & Mopper, K. (2008). Absorption spectral slopes and slope ratios as indicators of molecular weight, source, and photobleaching of chromophoric dissolved organic matter. *Limonology and Oceanography*, *53*(3), 955–969. https://doi.org/10.4319/lo.2008.53.3.0955

Hemes, K. S., Chamberlain, S. D., Eichelmann, E., Knox, S. H., & Baldocchi, D. D. (2018). A biogeochemical compromise: The high methane cost of sequestering carbon in restored wetlands. *Geophysical Research Letters*, *45*, 6081–6091. https://doi.org/10.1029/2018GL077747

Hemingway, J. D., Galy, V. V., Gagnon, A. R., Grant, K. E., Rosengard, S. Z., Soulet, G., et al. (2017). Assessing the blank carbon contribution, isotope mass balance, and kinetic isotope fractionation of the ramped pyrolysis/oxidation instrument at NOSAMS. *Radiocarbon*, *59*(01), 179–193. https://doi.org/10.1017/RDC.2017.3

Holgerson, M. A., & Raymond, P. A. (2016). Large contribution to inland water CO_2 and CH_4 emissions from very small ponds. *Nature Geoscience*, *9*(3), 222–226. https://doi.org/10.1038/ngeo2654

Hope, D., Dawson, J. J. C., Cresser, M. S., & Billett, M. F. (1995). A method for measuring free CO_2 in upland streamwater using headspace analysis. *Journal of Hydrology*, *166*(1-2), 1–14. https://doi.org/10.1016/0022-1694(94)02628-O

Hotchkiss, E. R., Hall Jr, R. O., Sponseller, R. A., Butman, D., Klaminder, J., Laudon, H., et al. (2015). Sources and control of CO_2 emissions change with the size of sreams and rivers. *Nature Geoscience*, *8*(9), 696–699. https://doi.org/10.1038/ngeo2507

Hua, Q., Barbetti, M., & Rakowski, A. Z. (2013). Atmospheric radiocarbon for the period 1950–2010. *Radiocarbon*, *55*(04), 2059–2072. https://doi.org/10.2458/azu_js_rc.v55i2.16177

Hulatt, C. J., Kaartokallio, H., Asmala, E., Autio, R., Stedmon, C. A., Sonninen, E., et al. (2014). Bioavailability and radiocarbon age of fluvial dissolved organic matter (DOM) from a northern peatland-dominated catchment: Effect of land-use change. *Aquatic Sciences*, *76*(3), 393–404. https://doi.org/10.1007/s00027-014-0342-y

Hulatt, C. J., Kaartokallio, H., Oinonen, M., Sonninen, E., Stedmon, C. A., & Thomas, D. N. (2014). Radiocarbon dating of fluvial organic matter reveals land-use impacts in boreal peatlands. *Environmental Science & Technology*, *48*(21), 12543–12551. https://doi.org/10.1021/es5030004

Hunter, W. R., Niederdorfer, R., Gernand, A., Veuger, B., Prommer, J., Mooshammer, M., et al. (2016). Metabolism of mineral-sorbed organic matter and microbial lifestyles in fluvial ecosystems. *Geophysical Research Letters*, *43*, 1582–1588. https://doi.org/10.1002/2016GL067719

Köhler, S., Buffam, I., Jonsson, A., & Bishop, K. (2002). Photochemical and microbial processing of stream and soil water dissolved organic matter in a boreal forested catchment in northern Sweden. *Aquatic Sciences*, *64*(3), 269–281. https://doi.org/10.1007/s00027-002-8071-z

Lawaetz, A. J., & Stedmon, C. A. (2009). Fluorescence intensity calibration using the Raman scatter peak of water. *Applied Spectroscopy*, *63*(8), 936–940. https://doi.org/10.1366/000370209788964548

Leach, J. A., Larsson, A., Wallin, W. B., Nilsson, M. B., & Laudon, H. (2016). Twelve year interannual and seasonal variability of stream carbon export from a boreal peatland catchment. *Journal of Geophysical Research: Biogeosciences*, *121*, 1851–1866. https://doi.org/10.1002/2016JG003357

Ledesma, J. L. J., Grabs, T., Bishop, K. H., Schiff, S. L., & Köhler, S. J. (2015). Potential for long-term transfer of dissolved organic carbon from riparian zones to streams in boreal catchments. *Global Change Biology*, *21*(8), 2963–2979. https://doi.org/10.1111/gcb.12872

Leith, F. I., Garnett, M. H., Dinsmore, K. J., Billett, M. F., & Heal, K. V. (2014). Source and age of dissolved and gaseous carbon in a peatland–riparian–stream continuum: A dual isotope (^{14}C and $\delta^{13}C$) analysis. *Biogeochemistry*, *119*(1–3), 415–433. https://doi.org/10.1007/s10533-014-9977-y

Levin, I., Kromer, B., & Hammer, S. (2013). Atmospheric $\Delta^{14}CO_2$ trend in Western European background air from 2000 to 2012. *Tellus Series B: Chemical and Physical Meteorology*, *65*(1), 20092. https://doi.org/10.3402/tellusb.v65i0.20092

Logue, J. B., Stedmon, C. A., Kellerman, A. M., Nielsen, N. J., Andersson, A. F., Laudon, H., et al. (2016). Experimental insights into the importance of aquatic bacterial community composition to the degradation of dissolved organic matter. *The ISME Journal*, *10*(3), 533–545. https://doi.org/10.1038/ismej.2015.131.

Loh, A. N., Bauer, J. E., & Canuel, E. A. (2006). Dissolved and particulate organic matter source-age characterization in the upper and lower Chesapeake Bay: A combined isotope and biochemical approach. *Limnology and Oceanography*, *51*(3), 1421–1431. https://doi.org/10.4319/lo.2006.51.3.1421

Mann, P. J., Eglinton, T. I., McIntyre, C. P., Zimov, N., Davydova, A., Vonk, J. E., et al. (2015). Utilization of ancient permafrost carbon in headwaters of Arctic fluvial networks. *Nature Communications*, *6*(1. https://doi.org/10.1038/ncomms8856), 7856.

Marwick, T. R., Tamooh, F., Teodoru, C. R., Borges, A. V., Darchambeau, F., & Bouillon, S. (2015). The age of river-transported carbon: A global perspective. *Global Biogeochemical Cycles*, *29*, 122–137. https://doi.org/10.1002/2014GB004911

McCallister, S. L., & del Giorgio, P. A. (2012). Evidence for the respiration of ancient terrestrial organic C in northern temperate lakes and streams. *Proceedings of the National Academy of Sciences of the United States of America*, *109*(42), 16,963–16,968. https://doi.org/10.1073/pnas.1207305109

Moore, S., Evans, C. D., Page, S. E., Garnett, M. H., Jones, T. G., Freeman, C., et al. (2013). Deep instability of deforested tropical peatlands revealed by fluvial organic carbon fluxes. *Nature*, *493*(7434), 660–663. https://doi.org/10.1038/nature11818

Müller, D., Warneke, T., Rixen, T., Müller, M., Jamahari, S., Denis, N., et al. (2015). Lateral carbon fluxes and CO_2 outgassing from a tropical peat-draining river. *Biogeosciences*, *12*(20), 5967–5979. https://doi.org/10.5194/bg-12-5967-2015

Murphy, K. R., Butler, K. D., Spencer, R. G. M., Stedmon, C. A., Boehme, J. R., & Aiken, G. R. (2010). Measurement of dissolved organic matter fluorescence in aquatic environments: An interlaboratory comparison. *Environmental Science & Technology*, *44*(24), 9405–9412. https://doi.org/10.1021/es102362t

Ohno, T. (2002). Fluorescence inner-filtering correction for determining the humification index of dissolved organic matter. *Environmental Science & Technology*, *36*(4), 742–746. https://doi.org/10.1021/es0155276

Page, S. E., Rieley, J. O., & Banks, C. J. (2011). Global and regional importance of the tropical peatland carbon pool. *Global Change Biology*, *17*(2), 798–818. https://doi.org/10.1111/j.1365-2486.2010.02279.x

Patel-Sorrentino, N. (2002). Excitation–emission fluorescence matrix to study pH influence on organic matter fluorescence in the Amazon basin rivers. *Water Research*, *36*(10), 2571–2581. https://doi.org/10.1016/S0043-1354(01)00469-9

Pickard, A. E., Heal, K. V., McLeod, A. R., & Dinsmore, K. J. (2017). Temporal changes in photoreactivity of dissolved organic carbon and implications for aquatic carbon fluxes from peatlands. *Biogeosciences*, *14*(7), 1793–1809. https://doi.org/10.5194/bg-14-1793-2017

Raymond, P. A., & Bauer, J. E. (2001). Riverine export of aged terrestrial organic matter to the North Atlantic Ocean. *Nature*, *409*(6819), 497–500. https://doi.org/10.1038/35054034

Raymond, P. A., Hartmann, J., Lauerwald, R., Sobek, S., McDonald, C., Hoover, M., et al. (2013). Global carbon dioxide emissions from inland waters. *Nature*, *503*(7476), 355–359. https://doi.org/10.1038/nature12760

Raymond, P. A., McClelland, J. W., Holmes, R. M., Zhulidov, A. V., Mull, K., Peterson, B. J., et al. (2007). Flux and age of dissolved organic carbon exported to the Arctic Ocean: A carbon isotopic study of the five largest arctic rivers. *Global Biogeochemical Cycles*, *21*, GB4011. https://doi.org/10.1029/2007GB002934

Reimer, P. J., Bard, E., Bayliss, A., Beck, J. W., Blackwell, P. G., Ramsey, C. B., et al. (2013). IntCal13 and Marine13 radiocarbon age calibration curves 0–50,000 years cal BP. *Radiocarbon*, *55*(04), 1869–1887. https://doi.org/10.2458/azu_js_rc.55.16947

Sierra, C. A., Müller, M., Metzler, H., Manzoni, S., & Trumbore, S. E. (2017). The muddle of ages, turnover, transit, and residence times in the carbon cycle. *Global Change Biology*, *23*(5), 1763–1773. https://doi.org/10.1111/gcb.13556

Spencer, R. G. M., Mann, P. J., Dittmar, T., Eglinton, T. I., McIntyre, C., Holmes, R. M., et al. (2015). Detecting the signature of permafrost thaw in Arctic rivers. *Geophysical Research Letters*, *42*, 2830–2835. https://doi.org/10.1002/2015GL063498

Stimson, A. G., Allott, T. E. H., Boult, S., & Evans, M. G. (2017a). Fluvial organic carbon composition and concentration variability within a peatland catchment—Implications for carbon cycling and water treatment. *Hydrological Processes*, *31*(23), 4183–4194. https://doi.org/10.1002/hyp.11352

Stimson, A. G., Allott, T. E. H., Boult, S., & Evans, M. G. (2017b). Reservoirs as hotspots of fluvial carbon cycling in peatland catchments. *Science of the Total Environment*, *580*, 398–411. https://doi.org/10.1016/j.scitotenv.2016.11.193

Tipping, E., Billett, M. F., Bryant, C. L., Buckingham, S., & Thacker, S. A. (2010). Sources and ages of dissolved organic matter in peatland streams: Evidence from chemistry mixture modelling and radiocarbon data. *Biogeochemistry*, *100*(1-3), 121–137. https://doi.org/10.1007/s10533-010-9409-6

Tittel, J., Büttner, O., Freier, K., Heiser, A., Sudbrack, R., & Ollesch, G. (2013). The age of terrestrial carbon export and rainfall intensity in a temperate river headwater system. *Biogeochemistry*, *115*(1–3), 53–63. https://doi.org/10.1007/s10533-013-9896-3

Vonk, J. E., Mann, P. J., Davydov, S., Davydova, A., Spencer, R. G. M., Schade, J., et al. (2013). High biolability of ancient permafrost carbon upon thaw. *Geophysical Research Letters*, *40*, 2689–2693. https://doi.org/10.1002/grl.50348

Vonk, J. E., Tank, S. E., Mann, P. J., Spencer, R. G. M., Treat, C. C., Striegl, R. G., et al. (2015). Biodegradability of dissolved organic carbon in permafrost soils and waterways: A meta-analysis. *Biogeosciences*, *12*(11), 8353–8393. https://doi.org/10.5194/bgd-12-8353-2015.

Walker, T. N., Garnett, M. H., Ward, S. E., Oakley, S., Bardgett, R. D., & Ostle, N. J. (2016). Vascular plants promote ancient peatland carbon loss with climate warming. *Global Change Biology*, *22*(5), 1880–1889. https://doi.org/10.1111/gcb.13213

Wohl, E., Hall, R. O., Lininger, K. B., Sutfin, N. A., & Walters, D. M. (2017). Carbon dynamics of river corridors and the effects of human alterations. *Ecological Monographs*, *87*(3), 379–409. https://doi.org/10.1002/ecm.1261

Xu, J., Morris, P. J., Liu, J., & Holden, J. (2018). Hotspots of peatlands-derived potable water use identified by global analysis. *Nature Sustainability*, *1*(5), 246–253. https://doi.org/10.1038/s41893-018-0064-6

Xu, S., Anderson, R., Bryant, C., Cook, G. T., Dougans, A., Freeman, S., et al. (2004). Capabilities of the new SUERC 5MV AMS facility for 14C dating. *Radiocarbon*, *46*(01), 59–64. https://doi.org/10.1017/S0033822200039357

Zhang, X., Bianchi, T. S., Cui, X., Rosenheim, B. E., Ping, C.-L., Hanna, A. J. M., et al. (2017). Permafrost organic carbon mobilization from the watershed to the Colville River Delta: Evidence from ^{14}C ramped pyrolysis and lignin biomarkers. *Geophysical Research Letters*, *44*, 11,491–11,500. https://doi.org/10.1002/2017GL075543